# Nanotechnology and the environment

Guillermina J. Gentile[1], María M. Fidalgo de Cortalezzi[2]
[1]*Department of Chemical Engineering, Instituto Tecnológico de Buenos Aires (ITBA), Buenos Aires, Argentina;*
[2]*Department of Civil and Environmental Engineering, University of Missouri, Columbia, MO, United States*

**CHAPTER OUTLINE**



## Nomenclature

**A** Hamaker constant
**BSA** Bovine serum albumin
**CCA** Constant charge approximation
**CCC** Critical coagulation concentration
**CNT** Carbon nanotubes
**CPA** Constant potential approximation
**EDL** Electrical double layer
**EPS** Extracellular polymeric substances
**IEP** Isoelectric point
**LSA** Linear superposition approximation
**NOM** Natural organic matter
**PZC** Point of zero charge

**ROS** Reactive oxygen species
**UV** Ultraviolet
**VOC** Volatile organic compound

# 1. NANOTECHNOLOGY IN THE NATURAL ENVIRONMENT

## 1.1 Introduction

Natural environments are chemically complex systems that include a myriad of inorganic and organic compounds that could potentially interact with nanomaterials on their surfaces leading to a change in their properties. Given that much of the characteristics of nanoparticles are dictated by their surface features and colloidal stability, interactions between nanomaterials and natural systems may result in modifications with effects on environmental risks and human health. Besides, prediction of these risks is hindered by the dynamic and stochastic nature of the environment. Multiple transformations can occur at the same time or successively, and the exposure is likely to happen in the long term and at very low concentrations [1].

The small size of natural and engineered nanoparticles and their high surface area to volume ratio determine different properties from those of the bulk material, as they offer a large number of atoms on the surface available to react with species present in the environment [2]. Therefore, properties and reactivity of nanomaterials make them dynamic in natural environments, affecting their transport, fate, and toxicity [1,3,4].

## 1.2 Transformations

When nanoparticles reach the aqueous environment, interactions with natural organic, inorganic, and biological colloids take place, as well as with dissolved compounds such as inorganic ions, humic, and nonhumic substances. These interactions may result in the formation of an adsorbed layer covering the nanoparticle surface [5,6], which in turn gives rise to new chemical and physical properties [7–14]. Stability of these particles will be therefore modified, inducing or preventing homo- and heteroaggregation and deposition processes [7,13,15], which are heavily dependent on the medium conditions, i.e., pH, ionic strength, dissolved ionic species [16–19]. Homoaggregation depends on ionic strength because ions compress the electrical double layer (EDL) enhancing attachment; at pH values close to the point of zero charge ($pH_{PZC}$), the energy barrier that prevents aggregation gets diminished, giving rise to net attractive forces.

Owing to this stability modification, the transport, fate, and influence on living species will be altered [14,20−22]. The analysis is further complicated by the fact that nanoparticles are often fabricated with coatings to provide special surface properties, and even if not intentionally, different synthesis routes impart their mark on the physicochemical characteristics of the product. As characteristics derived from nanoparticle surface composition are usually dominant over bulk-related ones, fabrication routes and coatings introduced in fabrication are critical to adsorption and aggregation processes.

Adsorption of different species such as proteins, dissolved natural organic matter (NOM), and metallic cations can take place on the nanomaterial surface and substantially modify its chemistry and charge. Not only nanoparticles will aggregate, but also these medium constituents will become concentrated in the solids. In this way, homoaggregation is expected to take place when high concentrations of nanoparticles are available; conversely, if the ratio between nanoparticles and colloids in the medium is low, heteroaggregation will be predominant [23]. Aggregation reduces the surface area, consequently decreasing the reactivity of the nanomaterials. Their toxicity will also be reduced, as it depends on the surface sites where the reactions can take place, and the larger particle dimension may be a barrier for uptake by organisms. Similarly, dissolution and degradation will also be hindered with augmented sizes, increasing the persistence in the environment.

Aggregation is regarded as an unfavourable outcome in nanoparticle-enabled products, and a large amount of effort has been devoted to the development of synthesis approaches that result in disperse and stable materials. During nanoparticle synthesis, different stabilizing agents—such as citrate, EDTA, thiolates, phosphine, carboxylates, and amines—are often used to prevent aggregation. When suspended in water, the interactions between colloids and nanoparticles are affected by the presence of these compounds; for example, citrate and EDTA bindings are relatively weak and easily replaced by proteins [6].

The adsorption of biomacromolecules, such as proteins and polysaccharides, affects aggregation, intake, distribution, and dissolution of the nanomaterials. NOM may replace ligands on the nanomaterial surface, giving rise to extended electrostatic repulsion and steric hindrance, therefore enhancing particle stability or, on the contrary, causing flocculation because of bridging among NOM-coated nanoparticles. Metal cations can adsorb on the surface itself or in the macromolecular coating, causing changes in charge and dissolution.

Proteins adsorb to nanoparticles forming a surrounding corona, and biological properties of the nanoparticles are therefore affected [24,25]. Coronas are heterogenous and formed by an inner layer (hard corona) composed of proteins of opposite charge to that of the particle and an outer layer (soft corona), which confers stability and contains proteins of the same charge as the nanoparticle. The inner layer exchanges proteins slowly with the surrounding medium, whereas the outer layer proteins, which are weakly bound, exchange faster [26,27]. The composition of the hard corona is determined by the size and surface charge of the nanoparticles and not by the properties of the bulk material [27]. As a result of the formation of the corona, the nanoparticles diminish their surface free energy, gaining thermodynamic stability [28]. The outer proteins undergo fast exchange with the medium, making the limit between the coated nanoparticle and the surroundings impossible to be defined in a precise way.

The types and amount of proteins that adsorb to the nanoparticles depend on hydrophobicity, surface area of the nanoparticles, concentration, and affinity for the nanoparticle—the first proteins to adsorb are those with high concentration and high association rate constant, but they are later replaced by those with higher affinity [25]. In this way, the interactions with the medium are not determined by the nanoparticle but by the particle and the corona formed by native-like or unfolded proteins, which will be in contact with living cells [25]. As the protein corona composition is kinetically controlled first, followed by conversion to equilibrium adsorption of high-affinity molecules, the nature of the transformation may also become time-dependent, as nanoparticle transformations in the environment "age."

Adsorbed proteins alter their structure because of the adsorption process and may enhance stability because of their globular shape and the resulting steric and electrostatic repulsion [29]. In recent studies [6,30,31], protein—nanoparticle adsorption was found to depend on the size and shape of the nanoparticles, as well as on the nature and charge of the protein, and that the stability of the nanoparticles increases when the ratio between protein and nanoparticle concentrations increases as well. Furthermore, it was concluded that the size of the nanoparticle not only determines the adsorption of a specific protein but also whether the changes in the protein's conformation are reversible or not.

The adsorption of proteins and polymers depends on the pH and electrolyte concentration of the medium. For $TiO_2$ nanoparticles, extracellular polymeric substance (EPS) adsorption is higher at lower pH values and at lower concentrations of NaCl, which influences the stability of the nanoparticles—in deionized water, aggregation only occurs at $pH < pH_{PZC}$, while at higher

values the amount of EPS has a minimal influence on the size of the aggregates. When ionic strength increases because of the addition of NaCl, aggregation increases as expected because of charge screening of the $TiO_2$ nanoparticles [32]. Furthermore, EPS is negatively charged at low pH values because of the extended deprotonation of functional groups with low pKa, such as carboxyl (pH 2−6), phospholipid (pH 2.4−7.2), and phosphodiester (pH 3.2−3.5), giving rise to electrostatic attraction with the positive $TiO_2$. At pH higher than the $pH_{PZC}$ of the $TiO_2$, repulsion originates between the positive nanoparticles and the further deprotonated EPS from hydroxyl (pH 9.0−10.0) and amino (pH 9.0−11.0) groups [33].

Hemoglobin adsorbed to gold nanoparticles capped with citrate provoked aggregation at pH 6; when pH was lowered, the size of the suspended aggregates decreased as the larger ones precipitated. A similar pattern is observed when the gold nanoparticles are stabilized using other capping agents, such as 6-mercaptopurine or ω-mercaptoundecanoic acid; aggregation takes place at the isoelectric point of the hemoglobin, which is a clear confirmation of the existence of the corona that changes the properties of the nanoparticles. Interestingly, the protein structure does not change while the nanoparticle−protein complex is stable, while at low pH changes on the secondary structure arise [34].

Hydrophobic nanoparticles, for example, carbon nanotubes (CNTs) and graphene, tend to adsorb not only biological and protein molecules but also NOM, polysaccharides, and tannic acid. These adsorbed compounds generate steric repulsion, which diminishes the rate of aggregation [35,36]. As stated before, the process depends on the size of the nanoparticles and conditions of the medium including, pH, and presence and concentration of dissolved electrolytes. When increasing the ionic strength, a change in the aggregation pattern of nanoparticles is observed when the critical coagulation concentration (CCC) is reached; the first step under unfavorable conditions is slow, later giving way to a rapid step under favorable conditions.

In the case of adsorbed NOM or alginate onto nanoparticles and when the concentration of an indifferent electrolyte such as NaCl is increased (up to 300 mM), a shift in the aggregation regime is not observed. This behavior indicates increased stability of the now coated nanoparticles; however, when $CaCl_2$ is present, the alginate nanoparticles may see their stability affected because of $Ca^{2+}$ bridging of alginate molecules [29]. The study showed that the effect of NOM and alginate was not as useful as that of protein bovine serum albumin (BSA) because of the globular shape of the latter, which enhances the long-range steric repulsion.

Numerous studies reported the influence of the medium on the stability of bare and NOM-coated nanoparticles. Graphene oxide nanoparticles are less stable when divalent cations, such as $Ca^{2+}$ and $Mg^{2+}$, are present in the medium. Cations are attracted to the negative surface, and electrostatic repulsion diminishes because of charge screening. Furthermore, as pH increases, aggregation is promoted because the carboxylic groups are deprotonated and then adsorb more divalent cations with the resulting surface charge increase and charge screening. The addition of NOM was found to enhance stability because of an increase in electrostatic and steric repulsion. This enhanced stability may be harmful to the environment and living species because the nanoparticles can be transported further distances in natural waters. The variation of pH showed that between levels of 5 and 7, the aggregation was refrained because of the presence of NOM when $Mg^{2+}$ was in the medium, but not when $Ca^{2+}$ was the cation. The steric hindrance originated from the presence of NOM overcame the reduction in electrostatic repulsion due to the $Mg^{2+}$. However, $Ca^{2+}$ could promote effective bridges between the adsorbed NOM due to specific interactions with the carboxylic and hydroxyl groups as well as its larger ionic radius. When pH increased from 7 to 9, no changes were observed in the behavior of the system in $Ca^{2+}$, but when $Mg^{2+}$ was present, aggregation did occur because of the desorption of NOM [37].

In another study [38], the presence of humic acid neither modified the size nor the zeta potential of silver nanoparticles because of the steric configuration of the adsorbed humic acid layer, which prevented aggregation.

The adsorption of tannic acid, with simpler chemical structure than humic acid, was investigated with the objective of stabilizing CNT in aqueous matrices [39]. Increasing particle size was shown to reduce deposition rates of nanoparticles in the presence of tannic acid because of the higher affinity between the acid and CNT at smaller sizes, clearly indicating a dependence based on surface properties. The nonpolar aromatic rings present in the tannic acid are prone to the formation of bonds with the CNT, and the polar hydroxyl and glucose ester will face the solvent. Thus, the nanoparticle surface is modified to become more polar and hydrophilic. When a high enough amount of tannic acid covers the nanoparticles, the thickness of the layer produces steric repulsion, and neither aggregation nor flocculation occurs.

Similar to the alkaline earth cations, heavy metals adsorb to nanoparticle surfaces as well. In a recent study [40], the effect of $Cr^{3+}$, $Pb^{2+}$, $Cu^{2+}$, $Cd^{2+}$, $Ag^{+}$ was studied, concluding that the adsorption modifies aggregation, stability and induces changes in morphology of graphene oxide

particles. These metallic cations bind to the surface, increase the surface charge, and diminish the EDL repulsion, giving rise to enhanced aggregation, which depends on the metal affinity for the nanomaterial. In the case of graphene oxide nanoparticles, it was concluded that this affinity increases when the element electronegativity is low. Moreover, water molecules in the solution form dipoles with the adsorbed ions, leading to a hydration shell that decreases the affinity of additional metal ions for the nanomaterial.

Dissolution of nanomaterials in natural waters enhances the uptake by living organisms, increasing nanotoxicity, which complements other mechanisms, e.g., oxidative stress [1,19]. The rate of dissolution is governed by nanomaterial characteristics, such as primary particle size, the degree of aggregation, shape, surface coating, and free surface area available for dissolution. Dissolution is also influenced by the medium pH, redox potential (e.g., silver nanoparticles that can be dissolved, thanks to the oxidation to $Ag^{+}$), ionic strength, and the presence of inorganic complexing ligands that lower the dissolution or organic ligands that, on the contrary, enhance dissolution [41,42]. Metal nanoparticles composed of zinc, copper, or silver are prone to combine dissolution with aggregation and sedimentation, depending on the time scales considered [41].

The speciation of the amphoteric ZnO, as it dissolves, is modified under different water chemistries: $Zn^{2+}$ predominates at low pH and $ZnO_2{}^{2-}$ at high pH and is enhanced by humic acid [43]. Anions $Cl^{-}$ and $SO_4{}^{2-}$ bind $Zn^{2+}$, thus dissolving greater amounts of ZnO [44]. The amount of dissolved zinc, when equilibrium is reached, increased with NOM content, as enhanced surface Zn binding was favored, and it depended on various NOM properties. Dissolution was enhanced by NOM with larger amounts of aromatic and carbonyl carbon content and with higher molecular weight but decreased with aliphatic carbon content and H/C ratio [41].

Copper-based nanoparticles, such as CuO and $Cu(OH)_2$, dissolved in aqueous media even when complex-forming ligands were present. However, this dissolution was diminished in the presence of NOM. Dissolution of zero-valent copper nanoparticles was accompanied in oxidizing media with the production of $Cu^{2+}$, which in turn formed precipitates of $Cu_2Cl(OH)_3$, CuO, and $Cu_3(PO_4)_3$, as well as with organic ligands [45].

For silver nanoparticles, it was found that dissolution occurred to a larger extent at high ionic strength [46]. Besides, when $Cl^{-}$ was found in the medium, it reacted with released $Ag^{+}$ precipitating AgCl, lowering the amount of $Ag^{+}$ in solution and favoring the dissolution of new silver nanoparticles. The influence of ultraviolet (UV) light was studied [47] and found that UV exposure produced changes in size, surface charge, and

chemistry, as well as dissolution rates of silver nanoparticles. Hydroxyl free radicals ($^{\bullet}OH$) created by UV light oxidized the surface of the nanoparticles. Furthermore, UV-exposed particles were retained to a larger degree in quartz sand columns and that more $Ag^{+}$ was released when nanoparticles did not undergo the aging process. Therefore, attached nanomaterials can be later released because of oxidation. Also, UVB irradiation caused greater aging, retention, and dissolution of the silver nanoparticles, compared with UVA.

Contrary to the results for ZnO nanoparticles in work by Jiang [48], other researchers found that the increase in humic acid content decreases the dissolution rate of silver nanoparticles because the adsorbed humic acid blocks the sites where Ag oxidizes to $Ag^{+}$, and the released $Ag^{+}$ may reduce back to Ag on the reducing sites offered by the humic acid [38]. Smaller silver nanoparticles have higher surface/volume ratio, which makes them energetically unfavorable, and therefore dissolved more readily than larger particles, which was enhanced at low pH [42]. Furthermore, the remaining silver nanoparticles were still spherical, did not aggregate, and did not undergo mineralogical changes, confirmed by X-ray diffraction, as metallic silver was present before and after the dissolution process.

The proposed oxidation mechanism [42] for the dissolution of silver nanoparticles included a first step where silver was oxidized by $O_2$ to $Ag_2O$ and the following step where the $Ag_2O$ reacted with $H^{+}$ to give $Ag^{+}$. The first step happens on the surface of the nanoparticles reached by dissolved oxygen. The layer of formed $Ag_2O$ dissolves as it is further oxidized by the protons of the medium, and therefore the process is pH-dependent.

## 1.3 Biological interactions

Nanomaterials have effects on existing microorganisms in soils and aqueous media. Adsorption of macromolecules, viruses, bacteria, and protozoa onto nanomaterials leads to surface changes that modify their reactivity and mobility. Interactions in the environment are inevitable, and reduction/oxidation reactions are essential in these types of transformations.

Silver nanoparticles can penetrate cell membranes, being harmful to microbes, fungi, algae, plants, and animals [42], and if cations are released, they can react with sulfur proteins, leading to cellular death [49]. Another pathway to cell damage via oxidative stress is the production of reactive oxygen species (ROS) (superoxide ion ($^{\bullet}O_2^{-}$), hydroxyl radicals ($^{\bullet}OH$), ozone ($O_3$), and hydrogen peroxide ($H_2O_2$)) by light irradiation [50].

When $TiO_2$ is UV irradiated, an electron in the valence band can be excited to a vacant conduction band, creating a hole. This electron/hole pair promotes the production of ROS, with the potential ability to harm bacteria, viruses, and fungi in water, air, or on surfaces because of photocatalytic reactions [51].

According to the review presented by Ref. [51], it has been proposed that antibacterial effects of $TiO_2$ are based on $^{\bullet}OH$, which is nonselective and has a short lifespan because it is an excellent oxidizing agent. Particles larger than 20 nm can adsorb onto bacterial cells and originate ROS that will oxidize the phospholipids of the cell membrane, while smaller particles can penetrate the bacterium and oxidize the coenzyme A as well as directly damaging the genome. Both the phospholipid membrane and the coenzyme A take an active part in the cellular respiration. Furthermore, UV irradiation causes the conversion of pyrimidine and purine to $CO_2$, $NH_3$, and $NO_3^-$. Bacterial death starts with the oxidative destruction of the cellular wall, followed by damage to the cytoplasmic membrane and internal components.

The mechanism of virus inactivation by UV-irradiated $TiO_2$ includes free surface-bound $^{\bullet}OH$, and other ROS, to a lesser scale. First, the capsid is damaged and then the genetic material is fragmented [52,53].

Only UV-irradiated $TiO_2$ presents fungicide activity, and it has been proved that not all fungi have the same response to photocatalytic activity because of complex differences between fungal groups—structure, chemical composition, and thickness of cellular wall [51].

## 1.4 Fate and transport

The first step to evaluate the risks that nanomaterials pose to the environment and living species is being aware of their sources and fate [54]. Nanoparticles originate from emissions from stationary (coal/oil/gas) boilers, incinerators, smelters, cooking, cigarettes, residential combustors, diesel/gasoline/LPG/CNG vehicles, metals in catalytic converters, and fuel cells [55]. Some of these particles may contaminate soils and waters as well as interact with living organisms [56,57].

Transport and fate of nanomaterials depend, to a larger extent, on aggregation and deposition. Large aggregates can migrate from soils and water to the plant kingdom, entering the food chain [58] and, as depicted in the previous section, many interactions occur among nanoparticles with macromolecules present in the medium, as well as transformations because of physical and chemical reactions.

To better understand the phenomena of aggregation and deposition, Boris Derjaguin and Lev Landau in 1941 and Evert Verwey and Theodoor Overbeek in 1948 developed a theory that analyzes the stability of colloid particles as well as the attachment between colloids and surfaces. The DLVO theory is based on the sum of two opposite forces, the van der Waals attraction and the EDL repulsion [59,60]. Attractive van der Waals forces are electromagnetic; transition dipoles originate for a very short period between two particles, regardless of the net charge. Therefore, this attraction depends on the geometry and properties of the particles and on properties of the medium in which they interact, given by the Hamaker constant (A). For aqueous media, Hamaker constants range between $3 \times 10^{-21}$ and $1 \times 10^{-19}$ J [61]. An EDL is developed when a charged particle is surrounded by counterions that are part of the electrolyte medium. These counterions face two opposite forces, attraction to be close to the particles and at the same time solvation tending to diffuse to the bulk. Therefore, an EDL is formed by the surface charge and the counterions. In this manner, when two similar-charged particles approach each other, both EDLs overlap creating a repulsion.

Owing to the electromagnetic nature of van der Waals dispersion forces, they are subject to retardation. Thus, a reduced correlation between oscillations in the interacting bodies and a smaller interaction is caused by the finite time of propagation. A characteristic wavelength of the interaction can be included, and it is usually 100 nm [62]. Retardation is important when the separation between the particles is of the same order of magnitude as the characteristic wavelength [61].

It is vital to know the value of the surface potential or surface charge to understand the EDL repulsion, but zeta potential, as a readily measurable variable, is used instead. Furthermore, it is not possible to have actual information of the dynamics of the double layer interaction; thus, calculations should be made using constant charge approximation (CCA) or constant potential approximation (CPA). For particles with fixed surface charge density, CCA is expected; the total diffuse layer charge does not vary, and when the two surfaces approach, this charge is compressed into a smaller volume making the charge density between the particles increase and thus the repulsion [63]. On the other hand, when the surface chemical equilibrium happens during the approach, CPA is expected; however, this is not feasible as the time for the encounter is too short. Nevertheless, Hogg, Healy, and Fuerstenau developed expressions using CPA [64] that are in agreement with exact results for low surface potentials [65]. When the separation distance is longer than the size of the particles, an intermediate option is the linear superposition approximation, which focuses on the

existence of a region between the two surfaces where the potential is small enough and follows the Poisson−Boltzmann equation, making it possible to sum the contributions from each surface [61].

Both van der Waals attraction and EDL repulsion energies may be calculated upon different expressions available in the literature, which are more straightforward to use than solving the Poisson−Boltzmann equation for the system. These expressions offer a wide range of possibilities according to the geometries of the particles and surfaces, such as a spherical or infinite plate.

The sum of the van der Waals attraction and the EDL repulsion potential energies gives the total or net potential energy. This total energy depends on the strengths of the attraction and the repulsion and is a function of the separation between the surfaces.

In the analysis of the total interaction potential energy (Fig. 2.1), three key points may be found. A primary minimum or deep energy well happens at very small distances, and where the particles are very unstable and therefore aggregate. An energy barrier or maximum arises at larger separations, where the repulsion between the two particles is greater than the attraction due to the values of zeta potentials and the ionic strength of the solution. Thus, aggregation is hindered. A special case arises if this maximum does not exist or disappears—the contact between both particles will be favored and a secondary minimum or shallow well may exist, where particles fast aggregate at longer distances. This type of profile is the result of the van der Waals attraction that is a function of the particle size and Hamaker constant and of the EDL repulsion which is determined by the particle size, zeta potential, ionic strength, and valence of the ions in the solution.

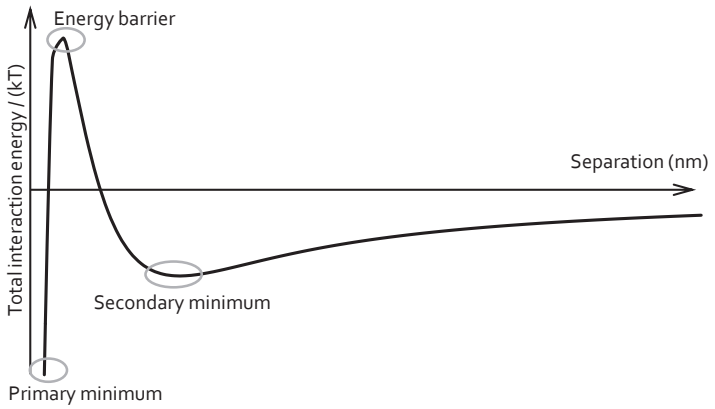


■ **FIGURE 2.1** Total interaction potential energy versus separation distance between the two surfaces, taking into consideration van der Waals attraction and electrical double layer repulsion.

Under no circumstances can the interaction energy at the primary minimum be considered to be infinite because a separation between the surfaces always exists as the particles are surrounded by water and hydrated ions.

The more ions present in the solution, the smaller the energy barrier and therefore the more enhanced collisions that lead to aggregation and then deposition. When the ion concentration of the solution reaches the CCC, the energy barrier no longer exists. DLVO theory predicts two different regimes; for concentrations below the CCC, the thickness of the EDL slowly decreases with increasing electrolyte concentration; but above the CCC, the EDL is completely suppressed and fast aggregation takes place no matter the salt concentration [66].

DLVO theory does not include Born short-range repulsion, hydration repulsion, hydrophobic attraction, steric interaction, or Lewis acid-base free interaction. Born repulsion between two atoms arises when their electron shells interpenetrate each other. However, in electrolyte solutions, these forces can be neglected because the hydrated ions prevent particles from being less than 3 nm apart. The origin of hydration repulsion is due to water molecules adsorbed onto the surfaces. Therefore, the particles first need to dehydrate to aggregate. Hydrophobic attraction needs to be taken into account in the case of surfaces without polar or ionic groups because water molecules will be prevented to adsorb and therefore will form fewer hydrogen bonds, having a less structured form than that of bulk molecules and tending to migrate to the bulk solution, favoring the contact between both particles. Steric interaction arises when particles have adsorbed polymers, which can act as bridges between particles promoting aggregation, or on the contrary, they can enhance stability when the adsorbed polymers repel themselves. Lewis acid-base interaction arises from the migration of electrons between the surfaces, adsorbed species, and the solvent.

DLVO theory does not account for surface roughness and heterogeneity. On the contrary, surfaces are thought of as possessing a homogenously defined geometry only comparable to a sphere or a plate. Hamaker constants are considered to depend only on the colloid material and the medium, but, in cases where counterions react with the particles, the measured or calculated constants are changed [66].

DLVO theory is not suitable for biological materials such as viruses and bacteria. These are soft, permeable particles that allow the exchange of water and electrolytes from the inside to the medium and vice versa [67]; consequently, the EDL is not limited to the outside of the particle but develops within the surface charge layer; in this context, the zeta potential importance and meaning may be questioned [68,69].

Despite these disadvantages, the results obtained by direct application of DLVO theory to nanosized objects are very useful in the estimation of the height of the energy barrier, which is indicative of the repulsion that arises between the two bodies in a specific medium. The depth of the secondary minimum determines the level of attraction at longer distances [70].

When a stream of nanoparticles is transported along a porous bed, interactions among them and with the granular medium take place. If repulsion is the net interaction between particles, as deposited particles increase in number, the deposition rate will be lowered because fewer attachment sites are available (blocking effect) [16], whereas when net attraction forces are present, the adsorbed particles on solid surfaces enhance the deposition rate (ripening effect) [71].

Nonelectrostatic interactions also exist. For instance, straining occurs when high electrolyte concentrations cause aggregation during the transport through porous beds rendering it more difficult for the particles to pass through the pores. Straining is a significant removal mechanism when the ratio between the particle and the collector diameters is below 0.05 or 0.005 according to different authors [72–74]. However, straining is still considered a removal mechanism even when the ratio between the diameter of the nanoparticle and the collector is less than 0.002 [75].

Many laboratory transport experiments were carried out for a wide variety of nanoparticles under different environmentally relevant conditions. The results of some studies are briefly reviewed below.

The influence of temperature was studied [76] via deposition of carboxyl-modified latex nanoparticles of 50 and 100 nm in diameter under moderate ionic strength of 10 and 30 mM. Deposition increased when the temperature was varied from 4 to 20°C because of the electrostatic nature of the deposition process that was enhanced by a decrease in the energy barrier.

Ionic strength in the aqueous matrix is a well-documented topic of research. Transport and retention of $TiO_2$ nanoparticles in saturated quartz sand was highly dependent on the concentration of the electrolyte (NaCl) solution. Retention increased when more salt was dissolved because of various mechanisms that coexist in this type of system. These mechanisms include electrostatic attraction between the nanoparticles and the clean granular bed surfaces, which were of opposite charge, an elevated salt concentration that promoted aggregation and thus straining, and attachment of incoming nanoparticles to those already deposited because of the attraction forces among them [20]. Breakthrough decrease with increasing ionic strength reveals the compression of the EDL, diminishing the repulsion between a

particle and a collector [77]. The same trend was observed in Ref. [16], where an increase in salt concentration (KCl) produced higher retention of the same nanoparticles. In Ref. [78], increased NaCl concentration, from 1 to 50 mM, proved to be useful to reduce $TiO_2$ mobility in both saturated and unsaturated river sand for the same reasons as stated before. The elution of $TiO_2$ and ZnO nanoparticles through quartz sand was highly diminished by the increase in ionic strength provided by NaCl or $CaCl_2$ [79], and nanoparticles of $TiO_2$, $Fe_3O_4$, CuO, and ZnO showed enhanced deposition onto glass beads when increasing ionic strength from 0 to 0.1 in NaCl [80], clearly indicating the electrostatic nature of the process. In Ref. [81], a different panorama was depicted; no net difference was observed in the high mobility of polyacrylic acid−coated $CeO_2$ nanoparticles through quartz sand when ionic strength, provided by $NaNO_3$, was increased from 100 to 500 mM, i.e., almost 100% elution, but a slightly higher deposition followed an increase up to 1000 mM.

In contrast, when the same particles were transported through loamy sand, the retention was considerably lower, and it increased with ionic strength because of the charge masking of the $Na^+$, leading to a high number of favorable deposition sites; however, blocking was present, and elution increased over time. In the same study, when divalent salts, such as $CaCl_2$ and $MgCl_2$, provided ionic strength, it was observed that the retention was much higher, and the loamy sand was more effective in capturing the particles than the quartz. The presence of divalent cations, especially $Ca^{2+}$, screens the surface charge and reduces the Debye length, reducing electrostatic repulsion and increasing aggregation and deposition onto the collector surface [21].

The influence of pH is of great importance because it determines whether the surface charge is positive or negative. At the pH values where nanomaterials and collectors have opposite charges, deposition is expected, which many researchers corroborated [77,78]. At neutral pH, $TiO_2$ transport was enhanced as a consequence of unfavorable conditions for deposition because both nanoparticles and quartz sand were negatively charged, while at lower pH, the retention was increased with increasing ionic strength [16]. Conversely, the significance of pH was low in the breakthrough of $TiO_2$, $Fe_3O_4$, CuO, and ZnO nanoparticles through glass beads [80].

The effect of nanoparticle concentration was also investigated by increasing the inlet concentration, which resulted in augmented elution in deionized water. Deposition due to attractive forces between the clean quartz and $TiO_2$ was expected and confirmed, but when no free collector area remained, which happened earlier at higher inlet concentrations, elution of

nanoparticles increased because of interparticle electrostatic repulsion. However, at 1 mM or higher NaCl concentration, no difference was found when increasing nanoparticle concentration [20]. On the other hand, increased elution for increased concentration was observed in 1 mM KCl at pH 5 in Ref. [16]. Another study [82] also showed that diminishing the input concentration of graphene oxide nanoparticles produced a decrease in the breakthrough curves through quartz sand due to a blocking effect.

Transport proved to be sensitive to flow characteristics. Increased flowrate reduced the retention of $TiO_2$ as a result of hydrodynamic forces leading to a blocking effect [16], and the retention of $TiO_2$, $Fe_3O_4$, CuO, and ZnO nanoparticles by glass beads was also diminished, due to complex factors because humic acid was present in the medium [80].

The deviations due to differences in granular media properties were examined [83]. $SiO_2$, $Al_2O_3$, and $TiO_2$ nanoparticles were highly retained in quartz sand, whereas poor retention was found in limestone for the three particles and in dolomite for $Al_2O_3$ and $TiO_2$. Transport through the porous bed was dependent on surface charge, nanoparticle stability, and grain roughness, showing the importance of electrostatic interactions, as well as straining process. The effectiveness of different beds (quartz sand, activated carbon, and diatomaceous earth) was analyzed [84] for nano-$TiO_2$ removal. Diatomaceous earth was the most effective, followed by activated carbon. The higher affinity exhibited by diatomaceous earth was the primary factor because the loading capacity was one order of magnitude higher compared to activated carbon and three orders when compared to sand. The inclusion of dispersive agents and organic compounds was also taken into account [84]. The addition of commercial dispersants decreased the retention of $TiO_2$ in granular media because of steric hindrance originated by the large size of the polymers. Lysozyme achieved higher retention because of the formation of aggregates that enhanced straining for filtration in quartz sand and activated carbon; conversely, lysozyme enhanced $TiO_2$ transport in diatomaceous earth, probably because of steric hindrance between the aggregates coated with the organic molecule. Glycine did not modify the transport and retention patterns in quartz sand, nor in activated carbon, whereas the retention was decreased in diatomaceous earth.

The size of the collector was also determinant of the degree of retention [82]. The elution of graphene oxide nanoparticles through a quartz sand column increased with increasing grain size as it can be explained by DLVO and classical colloid filtration theories. Straining offered a good explanation for the higher recovery rate of latex microspheres when the size of the quartz collectors decreased or the colloid radius increased [74].

The addition of organic matter was also investigated [85]. At acidic pH, negatively charged humic acid molecules adsorbed to $TiO_2$ as well as to the granular medium constituted by Fe oxyhydroxide coated quartz sand, and it contributed to aggregation and attachment because the repulsion from the positive charges on the $TiO_2$ and on the coating surface were in part decreased. At higher concentrations of humic acid, both charges were completely reverted, and attachment unfavored. Conversely, at alkaline pH, as the grain coating and the nanoparticles were negative, the adsorption of humic acid was not relevant. Thus, stability and attachment were not influenced.

In contrast with these results, another study showed that humic acid increased $TiO_2$, $Fe_3O_4$, CuO, and ZnO nanoparticles mobility, with little influence of pH [80]. The impact of cation valence on humic acid stabilized particles was investigated, and deposition rates decreased both in the presence of monovalent ($K^+$) and of divalent ($Ca^{2+}$) cations [21]. The retention of aqueous $C_{60}$, fullerol, and silver nanoparticles stabilized by citrate increased when the glass bead bed was coated with BSA and alginate, while polyvinylpyrrolidone-coated silver nanoparticles mobilization was augmented [86]. Hydrophobic forces explained the behavior of moderately hydrophobic aqueous $C_{60}$, which was further retained in highly hydrophobic BSA than in the less hydrophobic alginate. Increased attachment of fullerol and silver nanoparticles stabilized by citrate was explained as the result of hydrogen bonding. Steric repulsion between alginate and polyvinylpyrrolidone led to an enhanced breakthrough, whereas hydrophobic interaction could explain the behavior in BSA-coated beads.

The transport of nanoparticles through grains coated with a biofilm, constituted by EPSs, is a relevant mechanism as bacterial interfaces are often found in natural soils. Poly(vinylpyrrolidone)-stabilized silver nanoparticles were transported through saturated uncoated and coated with *Pseudomonas aeruginosa* PAO1 biofilm quartz sand, showing reduced retention in the latter, predominantly at low ionic strength, due to repulsive electrostatic forces and steric impediment [87]. The transport of aqueous $C_{60}$, fullerol, silver nanoparticles stabilized by citrate, and polyvinylpyrrolidone-coated silver nanoparticles in *Pseudomonas aeruginosa* and *Bacillus cereus* biofilm-coated glass beads was investigated [86], and researchers concluded that attachment increased in the presence of the biofilms for all particles, except for the polyvinylpyrrolidone-coated silver nanoparticles. Hydrophobic forces between aqueous $C_{60}$ and the hydrophobic region of the biofilm were responsible for the interaction. For fullerol and silver nanoparticles stabilized by citrate, increased attachment was due to hydrogen bonding or other associations with macromolecules of the biofilm. Steric repulsion between the polyvinylpyrrolidone and the polymers of the biofilm could originate steric repulsion, leading to the different behavior observed.

Cotransport with biological colloids such as bacteria and viruses, as well as inorganic nanoparticles, have been topics under study. For example, the presence of Gram-negative bacteria (*Pseudomonas aeruginosa* [20], *Escherichia coli* [21]) enhanced the retention of $TiO_2$ nanoparticles by quartz sand, due to straining, as large heteroaggregates were formed. Furthermore, a multilayer formed by $TiO_2$, which was attached to the grains, and incoming bacteria, attracted to the opposite-charged nanoparticles. Moreover, this retention increased with NaCl concentration, showing that EDL repulsion was a critical factor in the retention [20].

$TiO_2$ nanoparticles retention by a packed column was augmented by the presence of human adenoviruses because heteroaggregates were probably formed, and changes in flow velocity did not affect the mass recovery [88].

Cotransport of two types of inorganic nanoparticles showed that the transport of $TiO_2$ at pH 5 was not affected to a high degree by the presence of ZnO nanoparticles. However, at pH 7 a decrease and at pH 9 an increase in transport were noted; and that the transport of ZnO was decreased by the presence of $TiO_2$ at pH 5 and 7 and was increased pH 9 [79]. The authors hypothesized a probable competition between the nanoparticles for the deposition sites at pH 9.

## 2. NANOTECHNOLOGY IN ENVIRONMENTAL ENGINEERING SYSTEMS

### 2.1 Introduction

Applications of nanotechnology for air, water, and soil treatments tend to reduce concentration of a wide variety of species such as toxic gases, suspended organic compounds, heavy metals, and microbial pathogens, with the ultimate interest of avoiding human intake by absorption, inhalation, or ingestion [89]. Remediation processes need to be effective as well as green and economical. Opportunities including nanomaterials vary from adsorbents and membranes to sensors and disinfectants.

### 2.2 Adsorption processes

Due to the large specific surface area and reactivity, nanoparticles are ideal adsorbent materials and have been explored extensively for application in water treatment. However, their small size poses practical problems for their large-scale application, for example in a water treatment plant, and several strategies have been proposed to ease their transition from laboratory to industry, including aggregation, attachment on support materials, separation based on magnetism, and composite materials. Another potentially limiting

factor is the economics of the process, as the cost of some nanomaterials with excellent adsorption properties, such as graphene and graphene oxide, is still too high to be competitive for drinking water treatment processes. Also, concerns have been raised about the environmental impact of nanoparticles, when the full life cycle of the material is evaluated and potential toxicity, in the case that the small particles end up in treated wastewater as it is discharged to the natural environment or in drinking water.

Alternative synthesis methods for nanoparticles derived from waste materials, from agricultural, industrial or water treatment processes, have been explored to address these issues [90,91]. The waste-to-adsorbent approach adds value to an otherwise disposal problem but may lack in consistency of quality and quantity available; as well as in performance indicators such as adsorption capacity, reusability, etc. Herein, nanomaterials used as adsorbents for the removal of contaminants in water are discussed, based on their physicochemical properties as they relate to the adsorption process; their synthesis route, however, is out of the scope of this chapter.

Metal oxide nanoparticles play a crucial role as nanoadsorbents in water treatment. Examples include alumina, iron oxide and hydroxide, copper oxide, silica, zirconia, manganese oxide, titanium oxide, and some mixed metal oxides [92]. Surface areas vary depending on their fabrication method, from 30 to over 200 $m^2/g$. Metal oxides are known for their affinity toward cations in solution; heavy metal removal is one of the most extensively investigated application of metal oxide nanoparticles. It is noteworthy the role of nanoparticles in arsenic removal, in particular, iron oxide, titanium oxide, and alumina. The natural presence of arsenic in groundwater is a global public health issue, as millions of people are at risk due to elevated levels in their drinking water sources, both in urban and rural areas [93]. It is mainly in the latter situation where nanoparticles have mostly exhibited advantages over traditional treatment processes for arsenic removal, such as reverse osmosis. Several point-of-use-devices have been reported based on nanoadsorbents, including iron coated sand and activated carbon [94,95], amorphous and crystalline titania [96] and manganese-iron oxide [97]. Nano iron oxides are, by far, the most investigated materials for heavy metals' removal from water, with reports on goethite ($\alpha$-FeOOH), hematite ($\alpha$-$Fe_2O_3$), amorphous hydrous iron oxides, maghemite ($\gamma$-$Fe_2O_3$), and magnetite ($Fe_3O_4$) [98−101]. Significant attention has been devoted to magnetic nanoparticles such as iron oxide, manganese-iron oxide, and hydroxyapatite, that combine excellent adsorption capacity with ease of separation [92]. Superparamagnetic material properties of the nanomaterials allow the separation by low magnetic fields, obtaining concentrated exhausted adsorbent suspensions [102]. Other metals for which adsorption on oxide nanoparticles have been reported include lead, copper, cadmium, mercury, uranium, chromium, and selenium [103,104].

Overall, adsorption was found to be pH-dependent, with higher affinity of the As(V) anion below the PZC of the metal oxide surface, which has been exploited as a means to desorb the contaminant and regenerate the surface. In comparison, the ionic strength of the solution had little to no effect on the capacity, suggesting surface complexation and ligand exchange as the dominant mechanisms. With a few exceptions, the kinetics followed pseudo-second-order: a fast first step of heavy metal adsorption to the outer surface of the particle and a slower second step representing inner pore and intraparticle diffusion. This behavior is in good agreement with the well-studied process of cation adsorption on metal oxides: fast adsorption of divalent cations on iron oxides followed by a slower adsorption process for up to a few days has been reported before. In Refs. [105,106], the slow adsorption phase was modeled as a change in the extent of the outer sphere to inner sphere complexation over time, and conversion seemed to be the rate-limiting step in the adsorption of divalent cations. However, pore diffusion was also recognized in limiting access to internal adsorption sites for porous iron oxides [107].

Adsorption isotherms showed good agreement with Langmuir models, and in some instances also to Freundlich models. Mechanistically, the adsorption of heavy metals on metal oxide nanoparticles was found to be similar to that on the bulk material.

Nano metal oxides showed increased adsorption capacity for cations as the pH approached and passed the PZC of the material, but the opposite was observed for those elements present in the anionic form, such as As(V) and Cr(VI). These results may be mistakenly interpreted as a nonspecific (electrostatic) adsorption phenomenon. However, the presence of significant removal below and near the PZC of the solid, most noticeable for Pb(II) and Cu(II), is indicative of specific adsorption, where a net positive surface charge is not needed, but the presence of surface functional groups ($-OH_2^+$ and $-OH$) with the appropriate ligands for exchange suffices [107]. Specific adsorption on iron oxide surface involves interaction with deprotonated hydroxyl groups for cations and replacement of hydroxyl groups for anions, as described by Eqs. (2.1) and (2.2), respectively

$$\equiv XOH + Me^z \leftrightarrows \equiv XOM^{(z-1)} + H^+ \tag{2.1}$$

$$\equiv (XOH)_2 + Me^z \leftrightarrows \equiv (XO)_2M^{(z-2)} + 2H^+$$

$$\equiv XOH + L^- \leftrightarrows \equiv XL + OH^- \tag{2.2}$$

$$\equiv (XOH)_2 + L^- \leftrightarrows \equiv X_2L^+ + 2OH^-$$

for monodentate and bidentate mode of coordination, where ≡XOH represents the hydroxylated nanoparticle surface, $L^-$ the metal ion in its anionic form and $Me^{z+}$ the adsorbing cations.

The carbon-based family of nanomaterials has also been explored for adsorption in water treatment, and numerous studies are available in the literature regarding CNT, graphene, and graphene oxide nanoparticles. Compared to traditional adsorbent materials, carbon-based nanoparticles presented many advantages, such as higher adsorption capacity, ease of physical or chemical modification that allows for tunable adsorbents, antimicrobial properties, and reactivity, but their cost and scalability are still significant shortcomings. The pristine graphene and CNT surfaces are extremely hydrophobic, and therefore not suitable for water applications; however, surface oxidation that incorporates polar functional groups facilitates dispersion in water, while retaining the capacity to interact with organic pollutants via hydrophobic interactions. Tunable surface chemistries, hydrophobicity, and functionality allow diverse adsorption mechanisms: π−π interaction, covalent bonding, hydrophobic effects, and electrostatic interactions, and thus, target a wide array of adsorbates [108]. Surface functionalization plays a crucial role in the design of carbon-based adsorbents. In addition to chemical oxidation providing −OH and −COOH groups [109,110], it is possible to incorporate metals and metal oxides leading to composite materials that boost the properties of the inorganic nanoparticles such as iron oxides, alumina, titania, and silver [111−114]. The second effect of functionalization is the increase in hydrophilicity of the carbon nanoparticle that promotes dispersion in water and colloidal stability through electrostatic repulsion between nanoparticles and makes the surface more available for adsorption.

Additionally, the negatively charged groups are responsible for the adsorption of positively charged species, for example, heavy metals by electrostatic interactions. As the nanoparticle charge is derived from the protonation/deprotonation of surface groups, it is pH-dependent. Therefore, the colloidal stability and adsorption properties are also strongly dependent on pH and can be tuned by the appropriate choice of surface modifications. Carboxylic groups on the surface of CNTs and graphene oxide have pKa values in the range of 4−5; at lower pH, the material is expected to aggregate rapidly, resulting in larger highly porous particles [115]. However, most waters exhibit pH values above 5, where the developed negative surface charge promotes the adsorption of cations [116]. Ionic strength affects the process due to the decrease in the range of influence of electrostatic forces that improves attachment. The consequence of a high level of ionic strength is twofold: on one side, it increases the attachment efficiency

of electrostatically adsorbed contaminants, and therefore removal [117], but may also decrease the specific surface area if closed packed aggregates are formed, as in the case of graphene oxide particle stacking.

Carbon nanomaterials showed significant adsorption of organic compounds, with promising applications for the removal of NOM and synthetic organic pollutants such as pharmaceuticals and pesticides [118]. In addition to the electrostatic interactions mentioned, the hydrophobic fraction of the nanomaterial surface contributes to the removal of aromatic compounds through $\pi-\pi$ interactions [119], although functional groups were still recognized as essential [120] with water chemistry playing a substantial role in the organic chemical removal process.

The complexities of the effect of water chemistry on the adsorption of contaminants on carbon-based nanomaterials are not fully understood, and more research is needed to examine the process in realistic conditions [121] and assess its full potential. However, their high cost, compared to traditional adsorbents, and difficulties in recovery after adsorption, are the main drawbacks that need to be overcome before the materials can be deployed for large-scale applications.

## 2.3 Water filtration

Membrane processes in water treatment exhibit high separation along with no chemical or thermal consumption or secondary pollution [89]. Porous membranes are used in microfiltration and ultrafiltration, where the separation mechanism is screening. Mechanisms for contaminant removal by porous membranes in nanofiltration include screening, solution/diffusion, and exclusion. Dense membranes are employed in nanofiltration and reverse osmosis, where diffusion happens in the free volume among macromolecule chains that constitute the membrane because they do not have discernible pores. Examples of retained species by membranes are presented in Table 2.1 [122].

The addition of nanomaterials is an excellent solution to improve membrane characteristics, leading to high permeability, flux, selectivity, hydrophilicity, stability, as well as contaminant degradation, catalytic activity, and antifouling. Organic and biological fouling is responsible for flux decline, increasing operating costs, and diminishing the lifespan of both polymeric and ceramic membranes. Membranes are optimized to remove heavy metals by covalently attaching ceramic nanomaterials (hydrated alumina, alumina hydroxide, iron oxide) to the surface and compounds such as cyclodextrin to enhance the removal of organic molecules; while the incorporation of alumina, zirconium dioxide, silica, or zeolite nanoparticles improve their fouling resistance because they render the membrane more hydrophilic.

**Table 2.1** Examples of retained species in microfiltration (MF), ultrafiltration (UF), nanofiltration (NF), and reverse osmosis (RO).

| Species | Molar weight (Da) | Size (nm) | Membrane process | | | |
|---|---|---|---|---|---|---|
| | | | MF | UF | NF | RO |
| Yeast and fungi | | $10^3$–$10^4$ | X | | | |
| Bacteria | | 300–$10^4$ | X | X | | |
| Colloids | | 100–$10^3$ | X | X | | |
| Viruses | | 30–300 | X | X | | |
| Proteins | $10^4$–$10^6$ | 2–10 | | X | | |
| Polysaccharides | $10^3$–$10^6$ | 2–10 | | X | X | |
| Enzymes | $10^3$–$10^6$ | 2–5 | | X | X | |
| Simple sugars | 200–500 | 0.8–1 | | | X | X |
| Organic compounds | 100–500 | 0.4–0.8 | | | X | X |
| Inorganic ions | 10–100 | 0.2–0.4 | | | | X |

Moreover, titanium dioxide and zero-valent iron nanoparticles serve as photocatalysts, while silver nanoparticles inhibit biofilm growth [89]. The incorporation of bimetallic zero-valent Fe and Pt nanoparticles to polymeric membranes is suitable to reduce and degrade chlorinated organic compounds, while dendritic polymers can form ligands for metal cations, inorganic anions, and radionuclides, and size exclusion combined with oxidation by means of $TiO_2$ inclusion in the membrane material improves the removal and decomposition of organic compounds [123].

In summary, the addition of nanoparticles to the membrane matrix increases the interactions with the polymer or ceramic, resulting in enhanced desired properties, such as high permeability, selectivity, hydrophilicity, and robustness, as well as antifouling, antimicrobial, and photocatalytic activity [124].

## 2.4 Catalysis

Active sites are the principle of action in catalysis; therefore, working at the nanoscale is an excellent opportunity to increase surface area, which leads to faster reactions because more active sites are available.

Catalytic methods for removing organic pollutants and pathogens in water are based on UV radiation with or without oxidants. Homogenous photocatalysis uses $H_2O_2$ and dissolved Fe salts without irradiation (Fenton reaction) or with 600-nm light (photo-Fenton), while heterogenous

photocatalysis employs wide-bandgap semiconductors that are excited by light when $O_2$ is present [89].

$TiO_2$ nanoparticles degrade dyes under UV radiation, which is beneficial for those dyes resistant to biological treatments, though little effective under sunlight [125].

Photocatalysis with $TiO_2$ is used for disinfection at ambient temperature and pressure, exhibiting benefits such as low cost of the catalyst, completed mineralization without secondary products that affect the environmental quality, and potentially the use of solar radiation [51]. However, nanocrystalline powders agglomerate in water and are difficult to recover [89]. $TiO_2$ has antimicrobial properties because of its photocatalytic activity, producing ROS. For disinfection purposes, a more substantial activity can be obtained when this oxide is suspended because the contact with the microorganisms is enhanced, though immobilized nanoparticles onto quartz ($SiO_2$) exhibit higher photoactivity as the result of Si atoms diffusion [126]. Microorganisms such as fungi, bacteria, and viruses were targeted.

Photocatalysis is an option for killing and decomposing bacteria that are resistant to antibiotics and to UV light, which can be present in soils, water, sewage, food, and hospital environments. The presence of $TiO_2$ can reduce the viability and pathogenicity of bacteria. However, the antibacterial activity of $TiO_2$ needs UV light to be efficient, and therefore there is an ongoing search of dopants to enhance the activity under the visible spectrum. The process efficiency depends on various factors, such as bacterial strain, concentration, whether the cells are aggregated or disperse, resistance to temperature and pH, light source, irradiation time, type of $TiO_2$ employed, and $TiO_2$ loading [51]. Bacterial resistance is determined by those genes involved in the resistance against ROS [127]. A disadvantage is that some Gram-positive bacteria produce a superoxide dismutase enzyme that catalyzes the conversion of $^{\bullet}O_2^-$ to $H_2O_2$ and $O_2$ and a catalase enzyme that converts the $H_2O_2$ to $H_2O$ and $O_2$. Furthermore, some bacteria can recover damaged DNA and repair defective segments, though this ability can be suppressed by the conjunction of photocatalysis with the inclusion of $H_2O_2$ [51].

Viruses are more resistant than bacteria to conventional disinfection processes [128,129]. Enveloped viruses have an envelope formed by a lipid membrane and glycoproteins that are susceptible to denaturation by physical or chemical processes, turning them less resistant than naked (with no envelope) viruses. However, naked viruses have a greater tendency to be oxidized

by $^{\bullet}OH$ [126]. The mechanism for viral inactivation by $TiO_2$ under UV light includes a first step when free radicals ($^{\bullet}OH$ and $^{\bullet}O_2^-$) damage the protein capsid and a second one where the nucleic acid is fragmented [51−53]. Inactivation efficiency by photocatalysis depends on viral concentration, solution chemistry, light source, and on how long the viruses are subject to the process [51]. Inactivation rates obtained are very low, giving origin to metal doping to increase the photoactivity [130]. In natural soils, the presence of sand grains and BSA offers a protective layer for viruses, hampering virus inactivation produced by $TiO_2$ [51,126].

Fungi are composed of cells similar to those of higher organisms, rendering it more challenging to target only the fungi with no damage to other species; thus, photocatalysis is thought of as a method to address this problem, though the sensitivity of fungi is less than that of bacteria because of different chemical and structural composition [51]. The use of $TiO_2$ must be accompanied with UV light because $TiO_2$ in the dark has no antifungal effects [131].

Iron forms are also used in nanocatalysis. Hematite ($\alpha$-$Fe_2O_3$) absorbs light up to 600 nm and is stable in aqueous solutions at pH over 3; thus, it can be employed in photocatalysis and water treatment for elimination of organic compounds. The photocatalytic activity depends on composition, particle size, porosity, and local structures, but its efficiency is hampered by elevated recombination of electrons and holes, the low diffusion length of holes, and low conductivity [132]. Nano zero-valent iron (nZVI) is not toxic and used to degrade or eliminate heavy metals, anions, hydrocarbons, and halogenated organic compounds, having innocuous final products [133]. Nanoparticles made of iron and another metal (Pt, Ru, Rh, Ni, Co, Au, Cu, Ag) are also used to treat or remove pollutants, in particular, heavy metals, halogenated hydrocarbons, azo and nitro compounds, and oxyanions [133].

There is a wide range of other nanocatalysts employed in processes with environmental objectives. To cite a few, mesoporous silica nanomaterials are used in magnetic acid catalysis, hydrogenation catalysis, and photocatalysis; magnetic nanoparticles (Co, Fe, Ni, Cr, and their oxides) remove pesticides from groundwaters; two-metal layered hydroxides are often used in acid-base, redox, and photoelectrochemical catalysis [134]. Graphene is increasingly used in photocatalysis because of its high chemical stability, large surface area, and high adsorption capacity [135]. Catalytic and photocatalytic properties of gold nanoparticles serve to reduce or hydrogenate organic nitrogen molecules, generate hydrogen, oxidize CO, oxidize or degrade organics and dyes, and electrolytically oxidize alcohols, among other reactions [136].

Volatile organic compounds (VOCs) cause cancer, mutations, and teratogenesis [137]. Primary indoor air contaminants belong to aromatic, aldehyde, alkane, ketone, alcohol, and chlorocarbon families [138]. It is recommended indoor ventilation to control VOCs and different methods such as incineration, condensation, and adsorption are often used [139]. Adsorption and degradation of VOCs can be enhanced by the incorporation of nanoparticles as well as photoactivity [140].

When semiconductors are photoirradiated, an electron in the valence band can absorb a photon of appropriate energy and be excited to a vacant conduction band, creating a hole ($h^+$) in the former. The photocatalytic activity is determined by the defect disorder of the material, which is related to light absorption, charge transfer, and surface adsorption [141]. Both the excited electron and the hole promote the formation of $^{\bullet}OH$, which in the presence of humidity can oxidize VOCs, resulting in $CO_2$ (g) and $H_2O$ (g) [142]. This reaction has many intermediates, for example, acetone and benzoic acid, which are detrimental to the photoactivity of the semiconductor and more toxic than the parent compounds. Therefore, these can be harmful when the catalyst is regenerated if not done correctly and in an isolated area [139].

$TiO_2$ is the most used semiconductor for photocatalytic degradation of VOCs from indoor air [143], despite having the inconvenience of its poor adsorption capacity for VOCs and low surface area [144]. To increase photocatalytic activity, it is necessary to obtain a considerable amount of Ti—OH groups on the surface, thus the surface area should be maximized, preparing the catalyst in a thin layer together with its immobilization on a porous support, often made of silica, clays, zeolites, mesoporous materials, or carbon [143]. Mesoporous silica characteristics, such as physical stability, high surface area, hydrophobicity, and chemically inert and transparent to UV radiation, make it an attractive support material for this application [145—147].

Activated carbon has large surface area and adsorption capacity, making it fit for eliminating VOCs [148—150]. A drawback of this adsorbent is that airborne bacteria that deposit on its surface, efficiently multiply, and some VOCs are originated from bacterial metabolism, turning the activated carbon into a new source of biological and chemical contamination [151,152]. Considering that silver has antimicrobial properties [38,42,153], the addition of silver nanoparticles was proposed to address this problem, with due attention to the need to avoid aggregation because it prevents adequate contact with microbes as well as occludes the pores of the substrate and reduces adsorption capacity [152]. Their study concluded that a moderate loading of silver permitted to effectively mitigate bacteria attachment while adsorbing a VOC model like toluene to an acceptable degree.

Adsorption and oxidation by ozone on the surface of ferric hydroxide nanoparticles resulted in the efficient removal of VOCs obtained from cooking oil fumes [154]. The use of $Fe(OH)_3$ produced higher average $^{\cdot}OH$: $O_3$ ratio than for other iron oxide forms -β-FeOOH and α-$Fe_2O_3$- and in less ozone demand, thereby increasing the efficiency. Besides, the retention times for VOCs were short, and the residual ozone concentration was below 0.01 ppm.

## 2.5 Concluding remarks

Nanoparticles in the environment interact with colloids and dissolved compounds, favoring adsorption processes that modify surface chemistry, charge, and stability. Proteins that are adsorbed alter their structure and their globular shapes enhance stability. Both adsorbed proteins and NOM generate steric repulsion, diminishing aggregation and giving rise to different electrostatic interactions. Cations are attracted to negative nanoparticles lowering electrostatic repulsion because of charge screening. Aggregation depends on ionic strength, pH, and other suspended or dissolved species that may attach to the surface of the nanoparticles. Fate and transport are therefore modified by the chemical environment and influenced by the solubility of some nanomaterials in aquatic environments. The attachment of nanomaterials to microorganisms changes the reactivity and mobility of both species, and reduction and oxidation are important reactions taking place.

Nanomaterials have been extensively applied in water treatment as adsorbents due to properties such as large specific surface area and reactivity. Heavy metal removal is a significant goal that can be accomplished by employing metal oxide nanoparticles. In particular applications, water filtration using membrane-based technologies can be improved by the addition of nanomaterials, for example, to control fouling or to enhance metal removal. Catalysis is enhanced by the incorporation of nanoparticles providing an important number of active sites. The use of $TiO_2$ for photocatalytic disinfection has the benefit of operating at ambient temperature and pressure and does not generate secondary products. A wide range of nanocatalysts are also employed in environmental processes, such as adsorption and degradation of VOCs or the inclusion of iron-containing compounds in water treatments.

## REFERENCES


[1] Lowry GV, Gregory KB, Apte SC, Lead JR. Transformations of nanomaterials in the environment. Environ Sci Technol 2012;46:6893−9.

[2] Auffan M, Rose J, Bottero J-Y, Lowry GV, Jolivet J-P, Wiesner MR. Towards a definition of inorganic nanoparticles from an environmental, health and safety perspective. Nat Nanotechnol 2009;4:634.

[3] Ma S, Lin D. The biophysicochemical interactions at the interfaces between nanoparticles and aquatic organisms: adsorption and internalization. Environ Sci 2013;15:145−60.
[4] Schultz AG, Boyle D, Chamot D, Ong KJ, Wilkinson KJ, Mcgeer JC, Sunahara G, Goss GG. Aquatic toxicity of manufactured nanomaterials: challenges and recommendations for future toxicity testing. Environ Chem 2014;11:207−26.
[5] Diegoli S, Manciulea AL, Begum S, Jones IP, Lead JR, Preece JA. Interaction between manufactured gold nanoparticles and naturally occurring organic macromolecules. Sci Total Environ 2008;402:51−61.
[6] Kavok N, Grygorova G, Klochkov V, Yefimova S. The role of serum proteins in the stabilization of colloidal $LnVO_4:Eu^{3+}$ (Ln=La, Gd, Y) and $CeO_2$ nanoparticles. Colloid Surf, A 2017;529:594−9.
[7] Domingos RF, Tufenkji N, Wilkinson KJ. Aggregation of titanium dioxide nanoparticles: role of a fulvic acid. Environ Sci Technol 2009;43:1282−6.
[8] Domingos RF, Peyrot C, Wilkinson KJ. Aggregation of titanium dioxide nanoparticles: role of calcium and phosphate. Environ Chem 2010;7:61−6.
[9] Keller AA, Wang H, Zhou D, Lenihan HS, Cherr G, Cardinale BJ, Miller R, Ji Z. Stability and aggregation of metal oxide nanoparticles in natural aqueous matrices. Environ Sci Technol 2010;44:1962−7.
[10] French RA, Jacobson AR, Kim B, Isley SL, Penn RL, Baveye PC. Influence of ionic strength, pH, and cation valence on aggregation kinetics of titanium dioxide nanoparticles. Environ Sci Technol 2009;43:1354−9.
[11] Ottofuelling S, Von Der Kammer F, Hofmann T. Commercial titanium dioxide nanoparticles in both natural and synthetic water: comprehensive multidimensional testing and prediction of aggregation behavior. Environ Sci Technol 2011;45:10045−52.
[12] Zhang Y, Chen Y, Westerhoff P, Crittenden J. Impact of natural organic matter and divalent cations on the stability of aqueous nanoparticles. Water Res 2009;43: 4249−57.
[13] Dunphy Guzman KA, Finnegan MP, Banfield JF. Influence of surface potential on aggregation and transport of titania nanoparticles. Environ Sci Technol 2006;40: 7688−93.
[14] Petosa AR, Jaisi DP, Quevedo IR, Elimelech M, Tufenkji N. Aggregation and deposition of engineered nanomaterials in aquatic environments: role of physicochemical interactions. Environ Sci Technol 2010;44:6532−49.
[15] Mosley LM, Hunter KA, Ducker WA. Forces between colloid particles in natural waters. Environ Sci Technol 2003;37:3303−8.
[16] Chowdhury I, Hong Y, Honda RJ, Walker SL. Mechanisms of $TiO_2$ nanoparticle transport in porous media: role of solution chemistry, nanoparticle concentration, and flowrate. J Colloid Interface Sci 2011;360:548−55.
[17] Wang Y, Li Y, Pennell KD. Influence of electrolyte species and concentration on the aggregation and transport of fullerene nanoparticles in quartz sands. Environ Toxicol Chem 2008;27:1860−7.
[18] Thio BJR, Zhou D, Keller AA. Influence of natural organic matter on the aggregation and deposition of titanium dioxide nanoparticles. J Hazard Mater 2011;189:556−63.

[19] Zhang L, Li J, Yang K, Liu J, Lin D. Physicochemical transformation and algal toxicity of engineered nanoparticles in surface water samples. Environ Pollut 2016;211:132−40.
[20] Gentile GJ, Fidalgo De Cortalezzi MM. Enhanced retention of bacteria by $TiO_2$ nanoparticles in saturated porous media. J Contam Hydrol 2016;191:66−75.
[21] Chowdhury I, Cwiertny DM, Walker SL. Combined factors influencing the aggregation and deposition of nano-$TiO_2$ in the presence of humic acid and bacteria. Environ Sci Technol 2012;46:6968−76.
[22] Christian P, Von Der Kammer F, Baalousha M, Hofmann T. Nanoparticles: structure, properties, preparation and behaviour in environmental media. Ecotoxicology 2008;17:326−43.
[23] Emerson HP, Hart AE, Baldwin JA, Waterhouse TC, Kitchens CL, Mefford OT, Powell BA. Physical transformations of iron oxide and silver nanoparticles from an intermediate scale field transport study. J Nanoparticle Res 2014;16:2258.
[24] Monopoli MP, Aberg C, Salvati A, Dawson KA. Biomolecular coronas provide the biological identity of nanosized materials. Nat Nanotechnol 2012;7:779−86.
[25] Cedervall T, Lynch I, Foy M, Berggård T, Donnelly SC, Cagney G, Linse S, Dawson KA. Detailed identification of plasma proteins adsorbed on copolymer nanoparticles. Angew Chem Int Ed 2007;46:5754−6.
[26] Yang ST, Liu Y, Wang YW, Cao A. Biosafety and bioapplication of nanomaterials by designing protein-nanoparticle interactions. Small 2013;9:1635−53.
[27] Lundqvist M, Stigler J, Elia G, Lynch I, Cedervall T, Dawson KA. Nanoparticle size and surface properties determine the protein corona with possible implications for biological impacts. Proc Natl Acad Sci USA 2008;105:14265−70.
[28] Monopoli MP, Bombelli FB, Dawson KA. Nanobiotechnology: nanoparticle coronas take shape. Nat Nanotechnol 2011;6:11−2.
[29] Saleh NB, Pfefferle LD, Elimelech M. Influence of biomacromolecules and humic acid on the aggregation kinetics of single-walled carbon nanotubes. Environ Sci Technol 2010;44:2412−8.
[30] Piella J, Bastús NG, Puntes V. Size-dependent protein-nanoparticle interactions in citrate-stabilized gold nanoparticles: the emergence of the protein corona. Bioconjug Chem 2017;28:88−97.
[31] Kurtz-Chalot A, Villiers C, Pourchez J, Boudard D, Martini M, Marche PN, Cottier M, Forest V. Impact of silica nanoparticle surface chemistry on protein corona formation and consequential interactions with biological cells. Mater Sci Eng C 2017;75:16−24.
[32] Lin D, Story SD, Walker SL, Huang Q, Liang W, Cai P. Role of pH and ionic strength in the aggregation of $TiO_2$ nanoparticles in the presence of extracellular polymeric substances from *Bacillus subtilis*. Environ Pollut 2017;228:35−42.
[33] Martinez RE, Smith DS, Kulczycki E, Ferris FG. Determination of intrinsic bacterial surface acidity constants using a Donnan shell model and a continuous pKa distribution method. J Colloid Interface Sci 2002;253:130−9.
[34] Del Cano R, Mateus L, Sanchez-Obrero G, Sevilla JM, Madueno R, Blazquez M, Pineda T. Hemoglobin bioconjugates with surface-protected gold nanoparticles in aqueous media: the stability depends on solution pH and protein properties. J Colloid Interface Sci 2017;505:1165−71.

[35] Deonarine A, Lau BLT, Aiken GR, Ryan JN, Hsu-Kim H. Effects of humic substances on precipitation and aggregation of zinc sulfide nanoparticles. Environ Sci Technol 2011;45:3217−23.
[36] Domingos RF, Rafiei Z, Monteiro CE, Khan MAK, Wilkinson KJ. Agglomeration and dissolution of zinc oxide nanoparticles: role of ph, ionic strength and fulvic acid. Environ Chem 2013;10:306−12.
[37] Hua Z, Tang Z, Bai X, Zhang J, Yu L, Cheng H. Aggregation and resuspension of graphene oxide in simulated natural surface aquatic environments. Environ Pollut 2015;205:161−9.
[38] Linlin Z, Tanaka K. Dissolution of silver nanoparticles in presence of natural organic matter. Adv Mater Lett 2014;5:6−8.
[39] Lin D, Xing B. Tannic acid adsorption and its role for stabilizing carbon nanotube suspensions. Environ Sci Technol 2008;42:5917−23.
[40] Yang K, Chen B, Zhu X, Xing B. Aggregation, adsorption, and morphological transformation of graphene oxide in aqueous solutions containing different metal cations. Environ Sci Technol 2016;50:11066−75.
[41] Jiang C, Aiken GR, Hsu-Kim H. Effects of natural organic matter properties on the dissolution kinetics of zinc oxide nanoparticles. Environ Sci Technol 2015;49: 11476−84.
[42] Peretyazhko TS, Zhang Q, Colvin VL. Size-controlled dissolution of silver nanoparticles at neutral and acidic pH conditions: kinetics and size changes. Environ Sci Technol 2014;48:11954−61.
[43] Bian S-W, Mudunkotuwa IA, Rupasinghe T, Grassian VH. Aggregation and dissolution of 4 nm ZnO nanoparticles in aqueous environments: influence of ph, ionic strength, size, and adsorption of humic acid. Langmuir 2011;27:6059−68.
[44] Miao AJ, Zhang XY, Luo Z, Chen CS, Chin WC, Santschi PH, Quigg A. Zinc oxide-engineered nanoparticles: dissolution and toxicity to marine phytoplankton. Environ Toxicol Chem 2010;29:2814−22.
[45] Conway JR, Adeleye AS, Gardea-Torresdey J, Keller AA. Aggregation, dissolution, and transformation of copper nanoparticles in natural waters. Environ Sci Technol 2015;49:2749−56.
[46] Chambers BA, Afrooz ARMN, Bae S, Aich N, Katz L, Saleh NB, Kirisits MJ. Effects of chloride and ionic strength on physical morphology, dissolution, and bacterial toxicity of silver nanoparticles. Environ Sci Technol 2014;48:761−9.
[47] Mittelman AM, Fortner JD, Pennell KD. Effects of ultraviolet light on silver nanoparticle mobility and dissolution. Environ Sci 2015;2:683−91.
[48] Jiang X, Wang X, Tong M, Kim H. Initial transport and retention behaviors of ZnO nanoparticles in quartz sand porous media coated with *Escherichia coli* biofilm. Environ Pollut 2013b;174:38−49.
[49] Feng QL, Wu J, Chen GQ, Cui FZ, Kim TN, Kim JO. A mechanistic study of the antibacterial effect of silver ions on *Escherichia coli* and *Staphylococcus aureus*. J Biomed Mater Res 2000;52:662−8.
[50] Park HJ, Kim JY, Kim J, Lee JH, Hahn JS, Gu MB, Yoon J. Silver-ion-mediated reactive oxygen species generation affecting bactericidal activity. Water Res 2009; 43:1027−32.

[51] Markowska-Szczupak A, Ulfig K, Morawski AW. The application of titanium dioxide for deactivation of bioparticulates: an overview. Catal Today 2011;169: 249−57.
[52] Kashige N, Kakita Y, Nakashima Y, Miake F, Watanabe K. Mechanism of the photocatalytic inactivation of *Lactobacillus casei* phage Pl-1 by titania thin film. Curr Microbiol 2001;42:184−9.
[53] Cho M, Chung H, Choi W, Yoon J. Different inactivation behaviors of Ms-2 phage and *Escherichia coli* in $TiO_2$ photocatalytic disinfection. Appl Environ Microbiol 2005;71:270−5.
[54] Robichaud CO, Uyar AE, Darby MR, Zucker LG, Wiesner MR. Estimates of upper bounds and trends in nano-$TiO_2$ production as a basis for exposure assessment. Environ Sci Technol 2009;43:4227−33.
[55] Biswas P, Wu CY. Nanoparticles and the environment. J Air Waste Manag Assoc 2005;55:708−46.
[56] Klaine SJ, Alvarez PJJ, Batley GE, Fernandes TF, Handy RD, Lyon DY, Mahendra S, Mclaughlin MJ, Lead JR. Nanomaterials in the environment: behavior, fate, bioavailability, and effects. Environ Toxicol Chem 2008;27: 1825−51.
[57] Ray PC, Yu H, Fu PP. Toxicity and environmental risks of nanomaterials: challenges and future needs. J Environ Sci Health Part C Environ Carcinog Ecotoxicol Rev 2009;27:1−35.
[58] Bottero J-Y, Auffan M, Borschnek D, Chaurand P, Labille J, Levard C, Masion A, Tella M, Rose J, Wiesner MR. Nanotechnology, global development in the frame of environmental risk forecasting. A necessity of interdisciplinary researches. Compt Rendus Geosci 2015;347:35−42.
[59] Derjaguin B, Landau L. Theory of the stability of strongly charged lyophobic sols and of the adhesion of strongly charged particles in solutions of electrolytes. Acta Physicochim URSS 1941;14:733−62.
[60] Verwey EJW, Overbeek JTG. Theory of the stability of lyophobic colloids. J Colloid Sci 1955;10:224−5.
[61] Elimelech M, Gregory J, Jia X, Williams RA, Gregory J, Jia X, Williams RA. Particle deposition & aggregation. Woburn: Butterworth-Heinemann; 1995.
[62] Gregory J. Approximate expressions for retarded van der Waals interaction. J Colloid Interface Sci 1981;83:138−45.
[63] Gregory J. Interaction of unequal double layers at constant charge. J Colloid Interface Sci 1975;51:44−51.
[64] Hogg R, Healy TW, Fuerstenau DW. Mutual coagulation of colloidal dispersions. Trans Faraday Soc 1966;62:1638−51.
[65] Devereux OF, De Bruyn PL. Interaction of plane-parallel double layers. Cambridge, Mass: M.I.T. Press; 1963.
[66] Molina-Bolívar JA, Ortega-Vinuesa JL. How proteins stabilize colloidal particles by means of hydration forces. Langmuir 1999;15:2644−53.
[67] Ohshima H. Electrokinetic phenomena in a concentrated suspension of soft particles. Colloid Surf, A 2001;195:129−34.
[68] Duval JFL, Gaboriaud F. Progress in electrohydrodynamics of soft microbial particle interphases. Curr Opin Colloid Interface Sci 2010;15:184−95.

[69] Duval JFL, Ohshima H. Electrophoresis of diffuse soft particles. Langmuir 2006; 22:3533−46.
[70] Tripathi S, Champagne D, Tufenkji N. Transport behavior of selected nanoparticles with different surface coatings in granular porous media coated with *Pseudomonas aeruginosa* biofilm. Environ Sci Technol 2012;46:6942−9.
[71] Frimmel FH, Kammer FVD, Flemming H-C. Colloidal transport in porous media. Springer-Verlag Berlin Heidelberg; 2007.
[72] Hendry MJ, Lawrence JR, Maloszewski P. Effects of velocity on the transport of two bacteria through saturated sand. Gr Water 1999;37:103−12.
[73] Choi N-C, Kim D-J, Kim S-B. Quantification of bacterial mass recovery as a function of pore-water velocity and ionic strength. Res Microbiol 2007;158:70−8.
[74] Bradford SA, Bettahar M, Simunek J, Van Genuchten MT. Straining and attachment of colloids in physically heterogeneous porous media. Vadose Zone J 2004;3:384−94.
[75] Bradford SA, Yates SR, Bettahar M, Simunek J. Physical factors affecting the transport and fate of colloids in saturated porous media. Water Resour Res 2002; 38. 63-1−63-12.
[76] Sasidharan S, Torkzaban S, Bradford SA, Cook PG, Gupta VVSR. Temperature dependency of virus and nanoparticle transport and retention in saturated porous media. J Contam Hydrol 2017;196:10−20.
[77] Virkutyte J, Al-Abed SR, Choi H, Bennett-Stamper C. Distinct structural behavior and transport of $TiO_2$ nano- and nanostructured particles in sand. Colloid Surf, A 2014;443:188−94.
[78] Fang J, Xu M-J, Wang D-J, Wen B, Han J-Y. Modeling the transport of $TiO_2$ nanoparticle aggregates in saturated and unsaturated granular media: effects of ionic strength and pH. Water Res 2013;47:1399−408.
[79] Kumari J, Mathur A, Rajeshwari A, Venkatesan A, S S, Pulimi M, Chandrasekaran N, Nagarajan R, Mukherjee A. Individual and co transport study of titanium dioxide NPs and zinc oxide NPs in porous media. PLoS One 2015; 10:e0134796.
[80] Ben-Moshe T, Dror I, Berkowitz B. Transport of metal oxide nanoparticles in saturated porous media. Chemosphere 2010;81:387−93.
[81] Petosa AR, Öhl C, Rajput F, Tufenkji N. Mobility of nanosized cerium dioxide and polymeric capsules in quartz and loamy sands saturated with model and natural groundwaters. Water Res 2013;47:5889−900.
[82] Sun Y, Gao B, Bradford SA, Wu L, Chen H, Shi X, Wu J. Transport, retention, and size perturbation of graphene oxide in saturated porous media: effects of input concentration and grain size. Water Res 2015;68:24−33.
[83] Bayat AE, Junin R, Shamshirband S, Chong WT. Transport and retention of engineered $Al_2O_3$, $TiO_2$, and $SiO_2$ nanoparticles through various sedimentary rocks. Sci Rep 2015;5:14264.
[84] Rottman J, Platt LC, Sierra-Alvarez R, Shadman F. Removal of $TiO_2$ nanoparticles by porous media: effect of filtration media and water chemistry. Chem Eng J 2013; 217:212−20.
[85] Wu Y, Cheng T. Stability of n$TiO_2$ particles and their attachment to sand: effects of humic acid at different pH. Sci Total Environ 2016;541:579−89.

[86] Xiao Y, Wiesner MR. Transport and retention of selected engineered nanoparticles by porous media in the presence of a biofilm. Environ Sci Technol 2013;47: 2246−53.

[87] Mitzel MR, Tufenkji N. Transport of industrial PVP-stabilized silver nanoparticles in saturated quartz sand coated with *Pseudomonas aeruginosa* PAO1 biofilm of variable age. Environ Sci Technol 2014;48:2715−23.

[88] Syngouna VI, Chrysikopoulos CV, Kokkinos P, Tselepi MA, Vantarakis A. Cotransport of human adenoviruses with clay colloids and $TiO_2$ nanoparticles in saturated porous media: effect of flow velocity. Sci Total Environ 2017;598: 160−7.

[89] Ibrahim RK, Hayyan M, Alsaadi MA, Hayyan A, Ibrahim S. Environmental application of nanotechnology: air, soil, and water. Environ Sci Pollut Control Ser 2016;23:13754−88.

[90] Treviño-Cordero H, Juárez-Aguilar LG, Mendoza-Castillo DI, Hernández-Montoya V, Bonilla-Petriciolet A, Montes-Morán MA. Synthesis and adsorption properties of activated carbons from biomass of *Prunus domestica* and *Jacaranda mimosifolia* for the removal of heavy metals and dyes from water. Ind Crops Prod 2013;42:315−23.

[91] Cheng F, Luo H, Hu L, Yu B, Luo Z, Fidalgo De Cortalezzi M. Sludge carbonization and activation: from hazardous waste to functional materials for water treatment. J Environ Chem Eng 2016;4:4574−86.

[92] Dubey S, Banerjee S, Upadhyay SN, Sharma YC. Application of common nano-materials for removal of selected metallic species from water and wastewaters: a critical review. J Mol Liq 2017;240:656−77.

[93] WHO. Fact sheet [Online]. Available: http://www.who.int/mediacentre/factsheets/fs372/en/; 2017.

[94] Mostafa MG, Chen YH, Jean JS, Liu CC, Teng H. Adsorption and desorption properties of arsenate onto nano-sized iron-oxide-coated quartz. Water Sci Technol 2010;62:378−86.

[95] Zhu HJ, Jia YF, Wu X, Wang H. Removal of arsenite from drinking water by activated carbon supported nano zero-valent iron. Huanjing Kexue 2009;30: 1644−8.

[96] Jegadeesan G, Al-Abed SR, Sundaram V, Choi H, Scheckel KG, Dionysiou DD. Arsenic sorption on $TiO_2$ nanoparticles: size and crystallinity effects. Water Res 2010;44:965−73.

[97] Parsons JG, Lopez ML, Peralta-Videa JR, Gardea-Torresdey JL. Determination of arsenic(III) and arsenic(V) binding to microwave assisted hydrothermal synthetically prepared Fe3O4, $Mn_3O_4$, and $MnFe_2O_4$ nanoadsorbents. Microchem J 2009;91:100−6.

[98] Jiang W, Lv J, Luo L, Yang K, Lin Y, Hu F, Zhang J, Zhang S. Arsenate and cadmium co-adsorption and co-precipitation on goethite. J Hazard Mater 2013a; 262:55−63.

[99] Chen Y-H, Li F-A. Kinetic study on removal of copper(II) using goethite and hematite nano-photocatalysts. J Colloid Interface Sci 2010;347:277−81.

[100] Hu J, Chen G, Lo IMC. Removal and recovery of Cr(VI) from wastewater by maghemite nanoparticles. Water Res 2005;39:4528−36.

[101] Sabbatini P, Rossi F, Thern G, Marajofsky A, De Cortalezzi MMF. Iron oxide adsorbers for arsenic removal: a low cost treatment for rural areas and mobile applications. Desalination 2009;248:184−92.
[102] Li W, Mayo JT, Benoit DN, Troyer LD, Lewicka ZA, Lafferty BJ, Catalano JG, Lee SS, Colvin VL, Fortner JD. Engineered superparamagnetic iron oxide nanoparticles for ultra-enhanced uranium separation and sensing. J Mater Chem A 2016;4:15022−9.
[103] Thekkudan VN, Vaidyanathan VK, Ponnusamy SK, Charles C, Sundar S, Vishnu D, Anbalagan S, Vaithyanathan VK, Subramanian S. Review on nanoadsorbents: a solution for heavy metal removal from wastewater. IET Nanobiotechnol 2017;11:213−24.
[104] Hua M, Zhang S, Pan B, Zhang W, Lv L, Zhang Q. Heavy metal removal from water/wastewater by nanosized metal oxides: a review. J Hazard Mater 2012; 211−212:317−31.
[105] Jeon B-H, Dempsey BA, Burgos WD, Royer RA, Roden EE. Modeling the sorption kinetics of divalent metal ions to hematite. Water Res 2004;38:2499−504.
[106] Jeon B-H, Dempsey BA, Burgos WD, Royer RA. Sorption kinetics of Fe(II), Zn(II), Co(II), Ni(II), Cd(II), and Fe(II)/Me(II) onto hematite. Water Res 2003; 37:4135−42.
[107] Cornell RM, Schwertmann U. The iron oxides: structure, properties, reactions. Weinheim: Occurrences and Uses; 2004.
[108] Yang K, Xing B. Adsorption of organic compounds by carbon nanomaterials in aqueous phase: Polanyi theory and its application. Chem Rev 2010;110: 5989−6008.
[109] Kuila T, Bose S, Mishra AK, Khanra P, Kim NH, Lee JH. Chemical functionalization of graphene and its applications. Prog Mater Sci 2012;57: 1061−105.
[110] Smith B, Wepasnick K, Schrote KE, Cho HH, Ball WP, Fairbrother DH. Influence of surface oxides on the colloidal stability of multi-walled carbon nanotubes: a structure-property relationship. Langmuir 2009;25:9767−76.
[111] Pyrzyńska K, Bystrzejewski M. Comparative study of heavy metal ions sorption onto activated carbon, carbon nanotubes, and carbon-encapsulated magnetic nanoparticles. Colloid Surf, A 2010;362:102−9.
[112] Kim JD, Yun H, Kim GC, Lee CW, Choi HC. Antibacterial activity and reusability of Cnt-Ag and Go-Ag nanocomposites. Appl Surf Sci 2013;283:227−33.
[113] Guo J, Wang R, Tjiu WW, Pan J, Liu T. Synthesis of Fe nanoparticles@graphene composites for environmental applications. J Hazard Mater 2012;225−226:63−73.
[114] Gupta VK, Agarwal S, Saleh TA. Synthesis and characterization of alumina-coated carbon nanotubes and their application for lead removal. J Hazard Mater 2011;185: 17−23.
[115] Saleh NB, Pfefferle LD, Elimelech M. Aggregation kinetics of multiwalled carbon nanotubes in aquatic systems: measurements and environmental implications. Environ Sci Technol 2008;42:7963−9.
[116] Musico YLF, Santos CM, Dalida MLP, Rodrigues DF. Improved removal of lead(II) from water using a polymer-based graphene oxide nanocomposite. J Mater Chem A 2013;1:3789−96.

[117] Smith SC, Ahmed F, Gutierrez KM, Frigi Rodrigues D. A comparative study of lysozyme adsorption with graphene, graphene oxide, and single-walled carbon nanotubes: potential environmental applications. Chem Eng J 2014;240:147−54.
[118] Gao Y, Li Y, Zhang L, Huang H, Hu J, Shah SM, Su X. Adsorption and removal of tetracycline antibiotics from aqueous solution by graphene oxide. J Colloid Interface Sci 2012;368:540−6.
[119] Wang L, Zhu D, Duan L, Chen W. Adsorption of single-ringed N- and S-heterocyclic aromatics on carbon nanotubes. Carbon 2010;48:3906−15.
[120] Kim ES, Hwang G, Gamal El-Din M, Liu Y. Development of nanosilver and multi-walled carbon nanotubes thin-film nanocomposite membrane for enhanced water treatment. J Membr Sci 2012;394−395:37−48.
[121] Smith SC, Rodrigues DF. Carbon-based nanomaterials for removal of chemical and biological contaminants from water: a review of mechanisms and applications. Carbon 2015;91:122−43.
[122] Habert AC, Borges CP, Nobrega R. Processos de Separação por Membranas. 2006. Rio de Janeiro, Brasil.
[123] Ghasemzadeh G, Momenpour M, Omidi F, Hosseini MR, Ahani M, Barzegari A. Applications of nanomaterials in water treatment and environmental remediation. Front Environ Sci Eng 2014;8:471−82.
[124] Ying Y, Ying W, Li Q, Meng D, Ren G, Yan R, Peng X. Recent advances of nanomaterial-based membrane for water purification. Appl Mater Today 2017;7: 144−58.
[125] Santhosh C, Velmurugan V, Jacob G, Jeong SK, Grace AN, Bhatnagar A. Role of nanomaterials in water treatment applications: a review. Chem Eng J 2016;306: 1116−37.
[126] Syngouna VI, Chrysikopoulos CV. Inactivation of MS2 bacteriophage by titanium dioxide nanoparticles in the presence of quartz sand with and without ambient light. J Colloid Interface Sci 2017;497:117−25.
[127] Gogniat G, Dukan S. $TiO_2$ photocatalysis causes DNA damage via fenton reaction-generated hydroxyl radicals during the recovery period. Appl Environ Microbiol 2007;73:7740−3.
[128] Havelaar AH, Van Olphen M, Drost YC. F-specific RNA bacteriophages are adequate model organisms for enteric viruses in fresh water. Appl Environ Microbiol 1993;59:2956−62.
[129] Melnick JL, Gerba CP, Berg G. The ecology of enteroviruses in natural waters. Crit Rev Environ Contr 1980;10:65−93.
[130] Liga MV, Bryant EL, Colvin VL, Li Q. Virus inactivation by silver doped titanium dioxide nanoparticles for drinking water treatment. Water Res 2011;45:535−44.
[131] Maneerat C, Hayata Y. Antifungal activity of $TiO_2$ photocatalysis against *Penicillium expansum* in vitro and in fruit tests. Int J Food Microbiol 2006;107: 99−103.
[132] Li L, Wang M. Advanced nanomatericals for solar photocatalysis. In: Norena LE, Wang J-A, editors. Advanced catalytic materials−photocatalysis and other current trends. Rijeka: InTech; 2016.
[133] Kharisov BI, Kharissova OV, Dias HVR, Méndez UO, Fuente IGDL, Peña Y, Dimas AV. Iron-based nanomaterials in the catalysis. In: Norena LE, Wang J-A,

editors. Advanced catalytic materials—photocatalysis and other current trends. Rijeka: InTech; 2016.

[134] Sharma N, Ojha H, Bharadwaj A, Pathak DP, Sharma RK. Preparation and catalytic applications of nanomaterials: a review. RSC Adv 2015;5:53381—403.

[135] Zhou J, Jiao T, Zhang Q, Hu J. Preparation of functionalized graphene and gold nanocomposites—self-assembly and catalytic properties. In: Norena LE, Wang J-A, editors. Advanced catalytic materials—photocatalysis and other current trends. Rijeka: InTech; 2016.

[136] Priecel P, Adekunle Salami H, Padilla RH, Zhong Z, Lopez-Sanchez JA. Anisotropic gold nanoparticles: preparation and applications in catalysis. Chin J Catal 2016;37:1619—50.

[137] Fisher R, Summerson LA. Environmental technology verification report, Anest Iwata corporation W400-LV spray gun. Washington, DC: U.S. Environmental Protection Agency; 2004. EPA/600/R-04/154.

[138] Obee TN, Brown RT. $TiO_2$ photocatalysis for indoor air applications: effects of humidity and trace contaminant levels on the oxidation rates of formaldehyde, toluene, and 1,3-butadiene. Environ Sci Technol 1995;29:1223—31.

[139] Dhada I, Nagar PK, Sharma M, Gupta N. Photo-catalytic oxidation technology for VOC control: evaluation and risk characterization of intermediates of benzene degradation adsorbed on catalyst. Environ Eng Sci 2016;33:970—7.

[140] Dhada I, Nagar PK, Sharma M. Challenges of $TiO_2$-based photooxidation of volatile organic compounds: designing, coating, and regenerating catalyst. Ind Eng Chem Res 2015;54:5381—7.

[141] Pan X, Yang MQ, Fu X, Zhang N, Xu YJ. Defective $TiO_2$ with oxygen vacancies: synthesis, properties and photocatalytic applications. Nanoscale 2013;5:3601—14.

[142] Černigoj U, Štangar UL, Trebše P. Evaluation of a novel Carberry type photoreactor for the degradation of organic pollutants in water. J Photochem Photobiol A Chem 2007;188:169—76.

[143] Šuligoj A, Štangar UL, Ristić A, Mazaj M, Verhovšek D, Tušar NN. $TiO_2$-$SiO_2$ films from organic-free colloidal $TiO_2$ anatase nanoparticles as photocatalyst for removal of volatile organic compounds from indoor air. Appl Catal B Environ 2016;184:119—31.

[144] Šuligoj A, Štangar UL, Tušar NN. Photocatalytic air-cleaning using $TiO_2$ nanoparticles in porous silica substrate. Chem Paper 2014;68:1265—72.

[145] Kuwahara Y, Yamashita H. Efficient photocatalytic degradation of organics diluted in water and air using $TiO_2$ designed with zeolites and mesoporous silica materials. J Mater Chem 2011;21:2407—16.

[146] Qian X, Fuku K, Kuwahara Y, Kamegawa T, Mori K, Yamashita H. Design and functionalization of photocatalytic systems within mesoporous silica. ChemSusChem 2014;7:1528—36.

[147] López-Muñoz M-J, Grieken RV, Aguado J, Marugán J. Role of the support on the activity of silica-supported $TiO_2$ photocatalysts: structure of the $TiO_2$/Sba-15 photocatalysts. Catal Today 2005;101:307—14.

[148] Lillo-Ródenas MA, Cazorla-Amorós D, Linares-Solano A. Behaviour of activated carbons with different pore size distributions and surface oxygen groups for benzene and toluene adsorption at low concentrations. Carbon 2005;43:1758—67.

[149] Bastani A, Lee C-S, Haghighat F, Flaherty C, Lakdawala N. Assessing the performance of air cleaning devices—a full-scale test method. Build Environ 2010;45:143—9.
[150] Haghighat F, Lee C-S, Pant B, Bolourani G, Lakdawala N, Bastani A. Evaluation of various activated carbons for air cleaning—towards design of immune and sustainable buildings. Atmos Environ 2008;42:8176—84.
[151] Kuroda M, Yuzawa M, Sakakibara Y, Okamura M. Methanogenic bacteria adhered to solid supports. Water Res 1988;22:653—6.
[152] Pei L, Zhou J, Zhang L. Preparation and properties of Ag-coated activated carbon nanocomposites for indoor air quality control. Build Environ 2013;63:108—13.
[153] Dobrzynska MM, Gajowik A, Radzikowska J, Lankoff A, Dusinska M, Kruszewski M. Genotoxicity of silver and titanium dioxide nanoparticles in bone marrow cells of rats in vivo. Toxicology 2014;315:86—91.
[154] Lin B, Liaw S-L. Simultaneous removal of volatile organic compounds from cooking oil fumes by using gas-phase ozonation over $Fe(OH)_3$ nanoparticles. J Environ Chem Eng 2015;3:1530—8.